ADVANCED OPTICAL MATERIALS
www.advopticalmat.de

Low-Threshold Nanoimprinted Lasers Using Substructured Gratings for Control of Distributed Feedback

Emiliano R. Martins, Yue Wang, Alexander L. Kanibolotsky, Peter J. Skabara, Graham A. Turnbull, and Ifor D. W. Samuel**

Conjugated polymers combine high solid-state photoluminescence quantum yield (PLQY) with simple processing from solution. They have great potential as gain materials in low-cost miniature lasers with broad wavelength tuning.[1,2] Polymer lasers are commonly based on nanostructured polymer films for distributed feedback (DFB)[3–7] and photonic crystal resonators.[8] Such optical nanostructures in polymers can be fabricated by electron beam lithography,[9] or holography,[10] and could be simply replicated for volume production by direct embossing[11] or nanoimprint lithography.[12–14] However, a major challenge for practical polymer lasers is a need to lower the threshold density to enable the use of simple and cheap pumping systems, such as the recent breakthrough of a polymer laser pumped by an inorganic Light Emitting Diode (LED).[7,12] As well as improvements in gain properties, there is considerable scope to improve the optical nanostructure of the polymer.

Most polymer DFB lasers consist of a waveguide and a second order grating, in which second order diffraction leads to feedback, whilst first-order diffraction leads to output coupling. This type of resonator tends to provide excessive output coupling compared to feedback, resulting in high threshold. First order gratings avoid the problem of excessive output coupling but give edge emission,[6] which presents a problem for polymer lasers because it is difficult to make good facets and also loses the benefit of large-area surface emission. One promising approach is to use a mixed order grating as the cavity.[3,4] In this case, a few periods of a second order grating are inserted in the first order grating, thereby creating a defect cavity. Although the mixed order lasers retain the advantage of surface emission, this emission is limited to the defect. It would therefore be attractive to design large-area surface emitting cavities with low threshold.

Here, we present a new design of a nanopatterned polymer laser which uses a substructured grating to achieve low threshold lasing. The substructured grating is a second order grating with two different grooves (or ridges) in its unit-cell. We show that this extra feature allows complete control over the balance between feedback and output coupling, thereby having great influence on laser threshold. We show the potential of the approach by demonstrating low-threshold organic lasers fabricated using nanoimprint lithography. While demonstrated here for a conjugated polymer gain medium, the substructured grating design could also be employed in any kind of DFB laser.

As is well known from laser theory, laser threshold is strongly dependent on the resonator losses, including the output coupling.[15,16] The output coupling coefficient h_r and the feedback coupling coefficient h_f of second order DFB lasers depend on the grating parameter and operating wavelength as:[15]

$$h_r = \frac{2\pi\Lambda\Delta\varepsilon^2|\varepsilon_1|^2}{\lambda_0^4 K_x}\int_0^{GD} dx\left|\exp(iK_x x)\,\varphi(x)\right|^2$$
$$\text{and } h_f = \frac{\pi\Lambda\Delta\varepsilon\varepsilon_2}{\lambda_0^2}\int_0^{GD} dx\,|\varphi(x)|^2 \quad (1)$$

where Λ is the grating's period, λ_0 is the free-space wavelength, K_x is the propagation constant of the radiating field, φ is the transverse mode profile, GD is the groove depth, $\Delta\varepsilon$ is the dielectric contrast between grooves and ridges and ε_1 and ε_2 are the first and second Fourier orders, respectively. As is apparent from Equation (1), it is not easy to control h_r and h_f independently because they depend mostly on the same parameters, the only exceptions being the Fourier orders ε_1 and ε_2. For this reason, the Fourier properties of the cavity grating are of paramount importance in controlling the threshold of a DFB laser.

In conventional second order DFB lasers, the Fourier components ε_1 and ε_2 depend only on the filling factor of the grating. The lowest threshold in this case is achieved when ε_2 is maximized, i.e., for a filling factor of 75%, which has also been experimentally demonstrated by several groups.[17,18] The substructured gratings, in contrast, offer an extra degree of freedom that allows ε_2 to be arbitrarily greater than ε_1.

The operation of the substructured gratings can be formally described by the properties of the Fourier transform. The Fourier series of a periodic structure can be interpreted as a sampling of its unit-cell's Fourier transform, with the sampling position depending on the period. This property is represented in **Figure 1**a and b, which show a conventional second order grating in the real and Fourier spaces, respectively. The *sinc* function in Figure 1b (dashed red line) is the Fourier transform of the conventional second order grating unit-cell. The first and

E. R. Martins, Dr. Y. Wang, Dr. G. A. Turnbull, Prof. I. D. W. Samuel
Organic Semiconductor Centre
SUPA, School of Physics and Astronomy
University of St Andrews
North Haugh, St Andrews, KY, 16 9SS, UK
E-mail: gat@st-andrews.ac.uk; idws@st-andrews.ac.uk
Dr. A. L. Kanibolotsky, Prof. P. J. Skabara
WestCHEM
Departament of Pure and Applied Chemistry
University of Strathclyde
Thomas Graham Building, Glasgow, G1 1XL, UK

DOI: 10.1002/adom.201300211

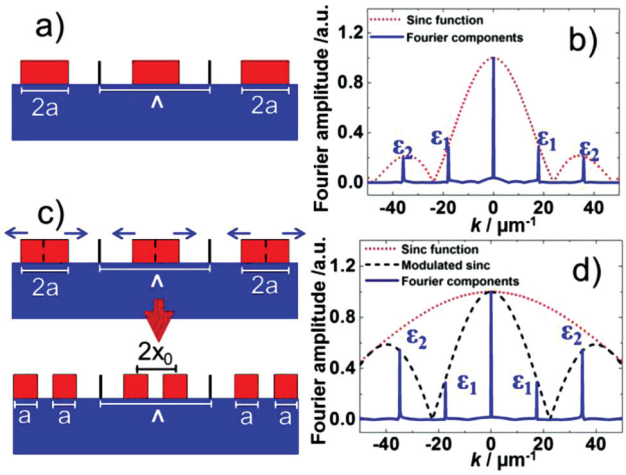

Figure 1. Operation of the substructured grating. (a)-(b) Conventional second order grating in real (a) and Fourier space. According to the properties of the Fourier transform, the harmonics (blue solid line) of the periodic structure can be interpreted as a sampling of the Fourier transform of the unit cell (dashed red line). Therefore, the second Fourier order ε_2 can never be greater than the first order ε_1. (c,d) The substructured gratings overcome this limitation by dividing the ridge in half and shifting the halves symmetrically (c). This shift induces a modulation in the Fourier transform of the unit cell (d) (dashed-dotted black line), which allows ε_2 to be made arbitrarily greater than ε_1.

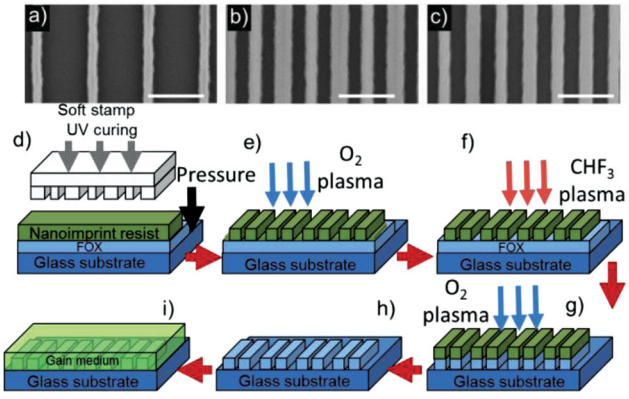

Figure 2. Fabrication process by nanoimprint lithography. a–c) SEM micrograph of reference, cavity 1 and cavity 2, respectively. All cavities have the same period of 350 nm (as shown by scale bar) but cavity 1 and cavity 2 have two grooves in one unit-cell. d) The soft stamp is first pressed against the nanoimprint resist during UV-curing. e) Next, the residual resist is removed by an O_2 plasma. f) The pattern is then transferred into the FOX layer by dry etching with CHF_3. g,h) In the next step, O_2 plasma is used again to remove the resist. i) Finally, the gain medium is spin-coated on the FOX grating cavity.

second orders of the Fourier series are shown as the solid blue line. Because these orders are obtained by sampling the *sinc* function, the first order amplitude ε_1 is always greater than the second order amplitude ε_2.

The substructured gratings overcome this limitation by imposing a modulation on the *sinc* function. The modulation is imposed in real space by dividing the ridge (or groove) width in half and shifting the halves symmetrically, as represented by the blue arrows in Figure 1c. The modulated sinc function is shown as the dashed-dotted black line in Figure 1d.

From the Fourier properties (see Supporting Information), a simple relation can be derived to express the ratio R between the second and first Fourier components, as shown in Equation (2), where a is the ridge width and x_0 is the spatial shift with respect to the axis of symmetry.

$$R = \frac{\varepsilon_2}{\varepsilon_1} = \cos\left(\frac{\pi a}{\Lambda}\right)\left[\cos\left(\frac{\pi 2x_0}{\Lambda}\right) - \sin\left(\frac{\pi 2x_0}{\Lambda}\right)\tan\left(\frac{\pi 2x_0}{\Lambda}\right)\right] \quad (2)$$

This ratio R can now be adjusted to any value ranging from zero (a conventional second order grating with 50% filling factor) to infinity (a first order grating).

The influence of the ratio R on the lasing properties is investigated experimentally by fabricating three cavities with different R and comparing their lasing properties. The fabricated cavities are: an optimized conventional second order grating (R = 0.7) as the reference cavity, a substructured second order grating with R = 9 (cavity 1) and a substructured second order grating with R = 22 (cavity 2). Scanning electron microscope (SEM) images of the cavities are shown in **Figure 2**a–c. All gratings have period of 350 nm but the substructured gratings have two grooves in one unit-cell. In cavity 1, the groove width is a = 60 nm and the spacing is $2x_0$ = 186 nm, resulting in R = 9, whereas in cavity 2, the groove width is a = 75 nm and the spacing is $2x_0$ = 179 nm, resulting in R = 22.

The cavities were fabricated by electron beam lithography on a master silicon wafer and transferred to a glass substrate through nanoimprint lithography, which is an emerging technology with potential of delivering low-cost mass production of nanostructures.[19] The fabrication process is shown in Figure 2d–i. First, the pattern on the silicon master is transferred to an intermediate soft-stamp. Then, the glass substrate is coated with Flowable Oxide (FOX), followed by spin-coating of the nanoimprint resist. The pattern is then transferred to the nanoimprint resist by pressing the soft-stamp against it during ultra-violet (UV) curing (Figure 2d). After demoulding the stamp, the residual resist is removed by O_2 plasma etching in a Reactive Ion Etcher (RIE) chamber (Figure 2e). The pattern is then transferred into FOX by CHF_3 dry etching (Figure 2f). After the resist is completely removed by O_2 plasma (Figure 2g,h), the gain medium is spin-coated on the top of the grating, thus forming the DFB cavity (Figure 2i).

In this work, we choose poly[2,5-bis(2′,5′-bis(2″-ethylhexyloxy)phenyl)-p-phenylene vinylene] (BBEHP-PPV) as the gain medium. This polymer has been reported previously with high optical gain coefficient and very low laser threshold fabricated using a first order DFB resonator.[6] We investigated the gain properties of the polymer by amplified spontaneous emission and observed that the gain narrowed and peaked at the wavelength of 533 nm. The optical feedback wavelength λ_{Bragg}, determined by Equation 3, is optimized to be at the maximal gain by choosing the appropriate grating period.

$$\lambda_{Bragg} = \frac{2\Lambda n_{eff}}{m} \quad (3)$$

Adv. Optical Mater. 2013,
DOI: 10.1002/adom.201300211

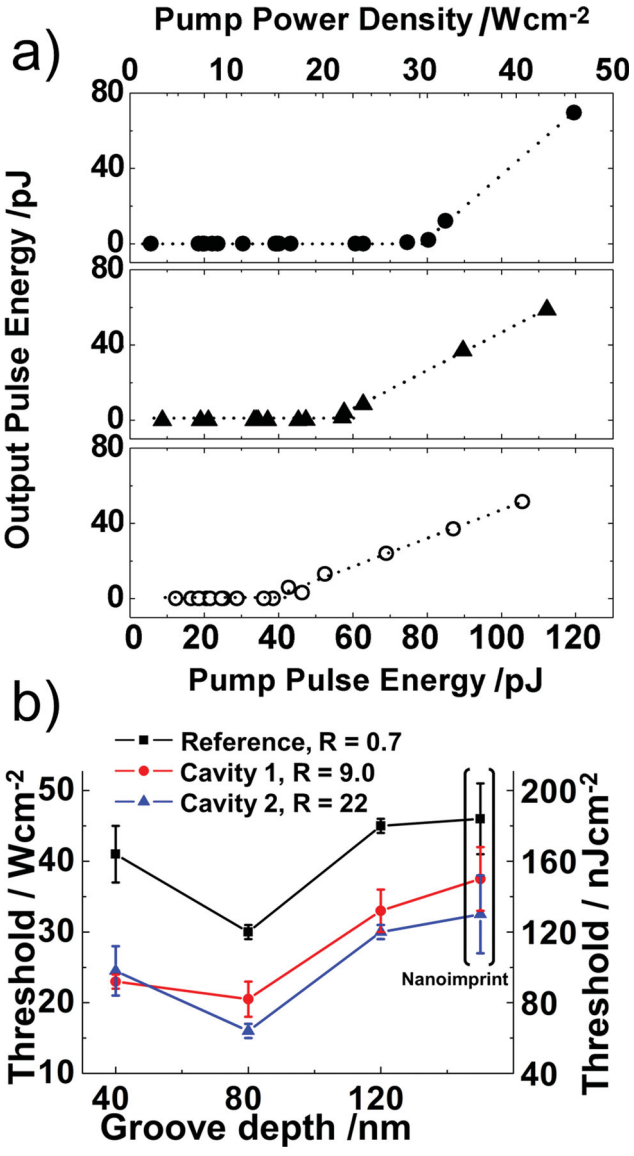

Figure 3. Laser Threshold properties. a) Output vs pump power density. The laser threshold is 31, 22 and 15 W/cm^2 for reference, cavity 1 and cavity 2, respectively. The grating depth is 80 nm for all cavities. b) Laser threshold dependence on grating depth. The cavities with higher *R* resulted in lower threshold in all cases.

In Equation (3), n_{eff} is the effective refractive index of the waveguided mode and *m* is an integer that represents the order of the scattering. In the case of second order surface-emitting lasers (*m* = *2*), the optimum period for laser at 533 nm is approximately 350 nm.

Figure 3a shows the laser threshold characterization for the reference, cavity 1 and cavity 2, all with a groove depth of 80 nm. The measured pump intensity thresholds are: 31 W/cm^2 for the reference, 22 W/cm^2 for cavity 1 and 15 W/cm^2 for cavity 2. According to Equation (1), the larger the value of *R*, the greater the feedback relative to output coupling. Thus, the lower threshold of cavities 1 (*R* = 9) and 2 (*R* = 22) compared to the reference cavity (R = 0.7) is a result of reduction in the output coupling in favour of the feedback coupling. This also explains why cavity 2 has the lowest threshold while the reference cavity has the highest threshold. The difference in the output coupling between the three cavities was observed experimentally from the laser slope efficiency. These results show that, by employing the substructured gratings, the laser threshold is reduced by almost half in comparison with the optimal conventional second order grating. Due to this lower output coupling, the threshold reduction is accompanied by a reduction in the power slope efficiency, which are 17%, 10% and 8.5% for the reference, cavity 1 and cavity 2, respectively. The laser spectra above and below threshold are shown in the Supporting Information.

In order to investigate the threshold dependence on grating depth, three different grating depths were fabricated by varying the CHF_3 etching time, and the results are shown in Figure 3b. The measurements show that all cavities are optimized for the same grating depth of 80 nm, and that grating profiles of larger *R* result in lower thresholds in all cases.

One of the main advantages of organic lasers is the possibility of fabricating large scale and low-cost lasers. The fabrication process here could be even simpler if the grating is made directly onto the nano-imprint resist.[12,14] In this case, the process consist of imprinting the nanoimprint resist (Figure 2d,e) and then spin coating the gain medium on the imprinted resist. In order to test the benefit of the substructured gratings in this architecture, referred to as "Nanoimprint" in Figure 3, the laser threshold was measured for the three different cavities, with groove depths of 80 nm. According to this measurement, the laser threshold is 30% lower in cavity 2 compared to the reference. The direct nanoimprint technique is simple, but yields a higher laser threshold than the gratings transferred into FOX, because the additional etch step allows optimisation of the groove depth and a stronger index contrast between the grating substrate and active layer.

Conventional second order DFB polymer lasers have been reported with low thresholds in a range of 100–300 W/cm^2.[1,20] The lowest laser threshold densities we are aware of in such lasers are in the range 30–40 W/cm^2,[18] comparable to our reference DFB laser threshold (30–45 W/cm^2). The substructured second order laser has allowed a further reduction of the reference threshold to 15 W/cm^2 (60 nJ/cm^2), approaching the reported *first* order DFB laser threshold of 10 W/cm^2 (40 nJ/cm^2), based on BBEHP-PPV.[6] The substructured lasers are also comparable with the very low laser threshold densities reported for polymer DFB lasers with mixed-order gratings; 4 W/cm^2 (36 nJ/cm^2) with a fluorene co-polymer gain medium[4] and 57 W/cm^2 (230 nJ/cm^2) with BBEHP-PPV.[14]

In order to gain insight into the properties of the substructured gratings acting as a laser resonator, we employed numerical simulations to investigate the effect of the enhancement of ε_2 over ε_1 on the cavity Quality factors (Q-factor). The Q-factor is the most relevant parameter for lasing operation and a higher Q-factor implies lower output losses. According to the simulations (see Supporting Information), compared to the reference, the Q-factor enhancement is 100 fold for cavity 1 and 500 fold for cavity 2. However, when experimentally determined extrinsic losses (mainly waveguide and self-absorption losses) are taken into account, the high Q-factor cavities are more

strongly affected. In this case, compared to the reference, the Q-factor enhancement is 18 for cavity 1 and 24 for cavity 2. This higher sensitivity of the high Q-factor cavity is a consequence of the longer propagation length of the photon inside the cavity. These observations indicate that the substructured gratings could provide even larger threshold reduction if the extrinsic losses are further reduced.

In conclusion, we have demonstrated a simple way of controlling the balance between feedback and output coupling in DFB resonators using substructured second order gratings. We demonstrated the potential of the substructured gratings by fabricating low-threshold nanoimprinted polymer lasers and found that the laser threshold can be almost halved compared with conventional second order gratings.

Experimental Section

The BBEHP-PPV lasers were optically pumped with 450 nm pulses (4 ns pulse width) at a repetition rate of 20 Hz from a Nd:YAG laser pumped optical parametric oscillator (OPO). The DFB laser emission was detected at an angle normal to the waveguide using the fibre coupled grating spectrograph with a highest resolution of 0.1 nm. The pump beam was focused to a 0.9 mm diameter spot (measured with a Coherent Inc. Beam Profiler at the position of the polymer films), which resulted in the excitation area of 0.64 mm^2.

Supporting Information

Supporting Information is available from the Wiley Online Library or from the author.

Acknowledgements

E. R. Martins and Y. Wang contributed equally to this paper.. We would like to thank the Scottish Universities Physics Alliance (SUPA) and the Engineering and Physical Sciences Research Council (EPSRC grant number EP/F059922/1 and EP/F05999X/1) for funding this project.

Received: May 13, 2013
Revised: June 9, 2013
Published online:

[1] S. Chenais, S. Forget, *Polym. Int.* **2012**, *61*, 390.
[2] a) G. J. Denton, N. Tessler, M. A. Stevens, R. H. Friend, *Adv. Mater.* **1997**, *9*, 547; b) F. Hide, M. A. DiazGarcia, B. J. Schwartz, M. R. Andersson, Q. B. Pei, A. J. Heeger, *Science* **1996**, *273*, 1833; c) M. D. McGehee, A. J. Heeger, *Adv. Mater.* **2000**, *12*, 1655; d) A. Camposeo, P. Del Carro, L. Persano, D. Pisignano, *Adv. Mater.* **2012**, *24*, Op221; e) J. Clark, G. Lanzani, *Nat. Photonics* **2010**, *4*, 438; f) D. Moses, *Appl. Phys. Lett.* **1992**, *60*, 3215; g) I. D. W. Samuel, G. A. Turnbull, *Chem. Rev.* **2007**, *107*, 1272.
[3] K. Baumann, T. Stoferle, N. Moll, R. F. Mahrt, T. Wahlbrink, J. Bolten, T. Mollenhauer, C. Moormann, U. Scherf, *Appl. Phys. Lett.* **2007**, *91*, 171108.
[4] C. Karnutsch, C. Pflumm, G. Heliotis, J. C. Demello, D. D. C. Bradley, J. Wang, T. Weimann, V. Haug, C. Gartner, U. Lemmer, *Appl. Phys. Lett.* **2007**, 90, 131104.
[5] a) G. Heliotis, R. D. Xia, G. A. Turnbull, P. Andrew, W. L. Barnes, I. D. W. Samuel, D. D. C. Bradley, *Adv. Funct. Mater.* **2004**, *14*, 91; b) S. Klinkhammer, X. Liu, K. Huska, Y. X. Shen, S. Vanderheiden, S. Valouch, C. Vannahme, S. Brase, T. Mappes, U. Lemmer, *Opt. Express* **2012**, *20*, 6357; c) T. Rabe, M. Hoping, D. Schneider, E. Becker, H. H. Johannes, W. Kowalsky, T. Weimann, J. Wang, P. Hinze, B. S. Nehls, U. Scherf, T. Farrell, T. Riedl, *Adv. Funct. Mater.* **2005**, *15*, 1188.
[6] A. Rose, Z. G. Zhu, C. F. Madigan, T. M. Swager, V. Bulovic, *Nature* **2005**, *434*, 876.
[7] Y. Yang, G. A. Turnbull, I. D. W. Samuel, *Appl. Phys. Lett.* **2008**, *92*, 163306.
[8] H. S. M. Notomi, T. Tamamura, K. Edagawa, *Phys. Rev. Lett.* **2004**, *92*, 1239061.
[9] R. Xia, G. Heliotis, P. N. Stavrinou, D. D. C. Bradley, *Appl Phys Lett* **2005**, *87*, 031104.
[10] L. M. Goldenberg, V. Lisinetskii, Y. Gritsai, J. Stumpe, S. Schrader, *Adv Mater* **2012**, *24*, 3339.
[11] a) C. Kallinger, M. Hilmer, A. Haugeneder, M. Perner, W. Spirkl, U. Lemmer, J. Feldmann, U. Scherf, K. Mullen, A. Gombert, V. Wittwer, *Adv. Mater.* **1998**, *10*, 920; b) M. Reufer, S. Riechel, J. M. Lupton, J. Feldmann, U. Lemmer, D. Schneider, T. Benstem, T. Dobbertin, W. Kowalsky, A. Gombert, K. Forberich, V. Wittwer, U. Scherf, *Appl. Phys. Lett.* **2004**, *84*, 3262.
[12] G. Tsiminis, Y. Wang, A. L. Kanibolotsky, A. R. Inigo, P. J. Skabara, I. D. W. Samuel, G. A. Turnbull, *Adv. Mater.* **2013**, *25*, 2826.
[13] a) E. B. Namdas, M. Tong, P. Ledochowitsch, S. R. Mednick, J. D. Yuen, D. Moses, A. J. Heeger, *Adv. Mater.* **2009**, *21*, 799; b) P. Del Carro, A. Camposeo, R. Stabile, E. Mele, L. Persano, R. Cingolani, D. Pisignano, *Appl. Phys. Lett.* **2006**, *89*, 201105; c) E. Mele, A. Camposeo, R. Stabile, P. Del Carro, F. Di Benedetto, L. Persano, R. Cingolani, D. Pisignano, *Appl. Phys. Lett.* **2006**, *89*, 131109.
[14] Y. Wang, G. Tsiminis, A. L. Kanibolotsky, P. J. Skabara, I. D. W. Samuel, G. A. Turnbull, *Opt. Express* **2013** , *21*, 14362.
[15] R. F. Kazarinov, C. H. Henry, *IEEE J. Quantum Electronics* **1985**, *21*, 144.
[16] A. E. Siegman, *Lasers*, University Sicence Books, California **1986**.
[17] a) G. F. Barlow, K. A. Shore, G. A. Turnbull, I. D. W. Samuel, *J. Opt. Soc. Am. B* **2004**, *21*, 2142; b) M. G. Ramirez, P. G. Boj, V. Navarro-Fuster, I. Vragovic, J. M. Villalvilla, I. Alonso, V. Trabadelo, S. Merino, M. A. Diaz-Garcia, *Opt. Express* **2011**, *19*, 22443.
[18] a) R. D. Xia, W. Y. Lai, P. A. Levermore, W. Huang, D. D. C. Bradley, *Adv. Funct. Mater.* **2009**, *19*, 2844; b) B. K. Yap, R. D. Xia, M. Campoy-Quiles, P. N. Stavrinou, D. D. C. Bradley, *Nat. Mater.* **2008**, *7*, 376.
[19] a) S. Y. Chou, P. R. Krauss, P. J. Renstrom, *Appl. Phys. Lett.* **1995**, *67*, 3114; b) L. J. Guo, *Adv. Mater.* **2007**, *19*, 495.
[20] a) G. Heliotis, R. Xia, D. D. C. Bradley, G. A. Turnbull, I. D. W. Samuel, P. Andrew, W. L. Barnes, *J. Appl. Phys.* **2004**, *96*, 6959; b) W. Y. Lai, R. D. Xia, Q. Y. He, P. A. Levermore, W. Huang, D. D. C. Bradley, *Adv. Mater.* **2009**, *21*, 355.